Published in final edited form as:
Semin Nucl Med. 2012 November ; 42(6): 423–432. doi:10.1053/j.semnuclmed.2012.07.001.

Development of Positron Emission Tomography β-Amyloid Plaque Imaging Agents

Chester A. Mathis, PhD[*,†], **N. Scott Mason, PhD**[*], **Brian J. Lopresti, BS**[*], and **William E. Klunk, MD, PhD**[‡,§]

[*]Department of Radiology, University of Pittsburgh School of Medicine, Pittsburgh, PA

[†]Department of Pharmaceutical Sciences, University of Pittsburgh School of Pharmacy, Pittsburgh, PA

[‡]Department of Psychiatry, University of Pittsburgh School of Medicine, Pittsburgh, PA

[§]Department of Neurology, University of Pittsburgh School of Medicine, Pittsburgh, PA

Abstract

For 100 years, β-amyloid (Aβ) plaques and neurofibrillary tangles (NFTs) have been recognized as the neuropathological hallmarks of Alzheimer's disease (AD), and their presence or absence could only be assessed postmortem using stains and dyes that identified these microscopic structures. Approximately 10 years ago, the first successful Aβ plaque–specific positron emission tomography (PET) imaging study was conducted in a living human subject clinically diagnosed with probable AD using the ^{11}C-labeled radiopharmaceutical Pittsburgh Compound B (PiB). Laboratory studies and preclinical evaluations to design PiB began a decade earlier than the first human PiB PET study and involved chemical modifications of different well-known dyes that bound specifically to the extended β-pleated sheets that comprise the fibrils of amyloid proteins such as Aβ plaques, NFTs, β-synuclein deposits, and prions. These preclinical studies were conducted in our laboratories at the University of Pittsburgh, starting with Congo red derivatives, followed by Chrysamine G derivatives, followed by X-series compounds, and finally with neutral derivatives of thioflavin-T. The in vitro and in vivo evaluations of the different derivatives as candidate PET radioligands for imaging Aβ plaques and neurofibrillary tangles in human brain are described in this review, along with the specific evaluation criteria by which the candidate radioligands were judged. Out of these studies came PiB, a PET radioligand that binds selectively and with high affinity to only fibrillar forms of Aβ. PiB has been used in many different human research protocols throughout the world and has demonstrated the usefulness of assessing the Aβ plaque status of subjects many years before the clinical diagnosis of probable AD. Recently, longer-lived ^{18}F-radiolabeled Aβ-selective radiopharmaceuticals have been developed. It is likely that the full clinical impact of these imaging agents will be realized by identifying presymptomatic subjects who would benefit from early drug treatments with future disease-modifying AD therapeutics.

Address reprint requests to Chester A. Mathis, PhD, PET Facility, Presbyterian University Hospital, B-938, 200 Lothrop Street, Pittsburgh, PA 15213. mathisca@upmc.edu.

GE Healthcare holds a license agreement with the University of Pittsburgh based on the technology described in this manuscript. C.A.M. and W.E.K. are coinventors of this technology and, as such, have a financial interest in this license agreement.

Early Efforts With Congo Red Derivatives

For many years, we struggled with manipulating the Congo red (CR) pharmacophore (Fig. 1) into a suitable positron emission tomography (PET) radiotracer to image β-amyloid (Aβ) plaques and hyperphosphorylated tau deposits in the form of neurofibrillary tangles (NFTs) in the brains of Alzheimer's disease (AD) subjects before death.[1–3] CR binds well to both of these aggregated proteins, which have been recognized as the postmortem hallmarks of AD from the time of Alzheimer himself.[4] Our efforts with CR fell short, primarily as a result of the poor brain entry of this class of compounds. Low brain uptake of CR after intravenous (iv) injection in animal studies likely resulted from the low lipophilicity of CR, which derived from its negative (−2) charge at physiological pH. In an effort to increase brain uptake, we examined radiolabeled derivatives of Chrysamine G (CG) (Fig. 1). CG bound with high affinity to both Aβ plaques and NFTs,[5] and CG had a higher lipophilicity than CR as measured by octanol/water partition coefficient (P) or octanol/buffered (pH 7.4) water distribution coefficient (D). Compounds with logD values in the range of 1–3 are known to cross the blood– brain barrier (BBB) more readily than compounds outside this range.[6,7] Although CG also displays a negative (−2) charge at pH 7.4, hydrogen bonding imparted by an adjacent -OH group of the salicylic acid moiety likely partially shields the negative charge and provides a compound with a much higher logD value than CR (logD of 1.8 for CG vs −0.2 for CR). Despite their higher logD values, radiolabeled derivatives of CG failed to provide significantly increased rodent brain entry compared with CR.[2] In an effort to decrease the molecular weight and complexity of CG, we synthesized a series of divinyl benzene compounds that we termed X compounds. Among the first X-series compounds was X-34[8] (Fig. 1), similar to CG in some respects but with a single central phenyl group and ring-bridging ethenyl groups rather than the azo groups of CG. Like CG, X-34 binds well to both Aβ plaques and NFTs and has a relatively high logD value (0.4), but does not readily cross the BBB. In an effort to increase logD and BBB penetration, we synthesized several hundred derivatives of X-34 and tested their binding affinities to synthetic Aβ fibrils. We focused on aggregated Aβ over tau binding because we had developed convenient Aβ(1–40) and Aβ(1–42) fibril assays[9] and did not have a readily available tau assay at that time. Out of these studies came the compound methoxy-X-04 (Fig. 1), which possessed a high logD value (2.6), reasonable BBB penetration, and moderately high affinity to Aβ fibrils.

Specific Evaluation Criteria for PET Amyloid Radioligands

During the evaluation of the many X-series derivatives, we considered what properties our ideal in vivo amyloid imaging agent should possess and compiled a list of these desired properties[3] (Table 1). It was clear that the radioligand should bind selectively to amyloid deposits, in the form of Aβ plaques or NFTs or both. It should bind to these deposits with high affinity; typical PET neuroreceptor-binding radioligands in use in the early 1990s such as [^{11}C]raclopride bound to their target protein site with equilibrium dissociation (K_d) or equilibrium inhibition (K_i) constants in the range of 1 nM.[10] Importantly, the amyloid-selective radioligand should readily cross the BBB, and this had proven to be a problem for CR and CG derivatives. A survey of the literature indicated that all the successful PET neuroreceptor radioligands in use in the mid-1990s entered the brain of rats a few minutes after iv tail-vein injection, with an uptake concentration value of ≥0.4% of the injected doses per gram of brain tissue (%ID/g). In mice, this value was ≥4%ID/g. Normalizing these values by the typical body mass (in kg) of the adult rodent provided a targeted minimum brain uptake value of 0.10(%ID/g)×kg or 1.0 standardized uptake value (SUV) unit.[3] In addition to good brain uptake, the PET radioligand should clear rapidly from non-target brain regions. We set the clearance half-time value of the radioligand from normal rodent brain at ≤30 minutes so that a reasonably high target-to-nontarget ratio could be achieved

within the relatively short half-lives of typical PET radionuclides such as ^{11}C (20.4 minutes) or ^{18}F (109.8 minutes). Because PET follows the radionuclide distribution (whether incorporated in the parent compound or a radiometabolite), we wanted to ensure that radiolabeled metabolites of the radioligand were not present in the brain, thereby complicating the pharmacokinetic analysis of the radioligand in the brain. Finally, we desired to demonstrate the usefulness of the radioligand in the newly devised transgenic mouse models of AD.[11]

None of the X-series compounds met all of these acceptance criteria. One of the best compounds from this series was methoxy-X-04, and its brain uptake at 2 minutes and binding affinity to Aβ(1–40) fibrils were below the minimally acceptable values we had set (Table 1).[3] Hence, we began to consider other amyloid-binding pharmacophores. However, before dismissing the CR and X-series of compounds as good in vivo PET amyloid imaging agents, it is important to point out that a variety of useful outcomes derived from this early work with CG and X compounds. The 3 best known are as follows: (1) CG may protect from Aβ-induced neurotoxicity and has been explored as a γ-secretase modulator[12,13]; (2) X-34 is a highly fluorescent compound8 that is remarkably sensitive for AD pathology in histologic applications[14]; and (3) methoxy-X-04 has proven to be very useful for in vivo imaging in 2-photon microscopy applications in transgenic mouse models of AD,[15–18] as well as in prion disease.[19] It is also worth pointing out that X-34 is the basic structural backbone for (trans,trans)-1-bromo-2,5-bis-(3-hydroxycarbonyl-4-hydroxy)styryl-benzene or “BSB,” a compound that differs from X-34 only by the addition of 1 bromine atom.[20] BSB, like CR, has been shown to bind to Aβ oligomers (although at solution concentrations many times higher than those attained in PET studies).[21]

Evaluation of Thioflavin-T Analogs

After investing 6 years evaluating several hundred CR and X-series derivatives, our transition away from these compounds began in late 1999. We considered several other amyloid-binding pharmacophores (Fig. 2), and settled on exploring neutral lipophilic thioflavin-T derivatives for several reasons.[22] Amyloid-binding Aβ and tau peptides and antibodies do not have high BBB penetration and were eliminated as candidates. Thioflavin-S is a mixture of several different compounds, and the most abundant compound in the mixture has 2 positive charges and a negative charge at pH 7.4 (Fig. 2). Thioflavin-T is a well-characterized relatively small molecule, and has only 1 positive charge. We therefore chose to synthesize neutral derivatives of thioflavin-T (termed benzothiazole-aniline or BTA derivatives) and assess their BBB penetration and binding affinities to Aβ plaques and NFTs (Fig. 3). Radiolabeling many of these derivatives with ^{11}C for further evaluations proved to be straightforward via methylation of amino or hydroxyl groups with -[^{11}C]CH_3 to form N-methyl amines or methoxy derivatives. These compounds were injected into control mice, and their brain uptake at 2 minutes was evaluated (Fig. 4).[23,24] Of the first 11 ^{11}C -labeled BTA compounds evaluated in mice, 10 exceeded our minimum brain uptake requirement of 1.0 SUV at 2 minutes after iv injection. Although many of the BTA compounds quickly proved to be efficient in penetrating the BBB, an unresolved question was the effect on Aβ and tau binding of the removal of the N-methyl group from the nitrogen of the heterocyclic benzothiazole ring to form the neutral BTA derivatives. Fortunately, the neutral BTA derivatives bound to Aβ(1–40) fibrils with much higher affinity than the parent thioflavin-T compound (Fig. 5),[22,24] and these neutral BTA derivatives bound with very low affinity to aggregated tau. We then synthesized and evaluated several hundred BTA derivatives, and a representative structure–affinity assessment is shown in Figure 6. Several of the BTA derivatives bound to Aβ(1–40) fibrils, with binding affinities approximately equal to the desired value of 1 nM. The next important criterion was to determine the clearance rate of radiotracer from normal rodent brain. This was accomplished relatively easily by comparing

the 2-minute brain uptake values in one group of normal mice with the 30-minute brain uptake values in another group of normal mice.[23] The ratio of these 2 values provides an index of the 30-minute clearance rate: a ratio of 2 indicates approximately a 30-minute clearance half-time and a ratio of 8 indicates approximately a 10-minute clearance half-time. The 2 minute-to-30 minute brain uptake ratios for several BTA compounds are shown in Fig. 7, and it is evident that the 6-OH N-HCH_3 derivative (termed 6-OH-BTA-1) possessed a relatively high 2 minute-to-30 minute ratio of 11. This indicated an in vivo clearance half-life of this compound of approximately 6 minutes from normal mouse brain, and, combined with a K_i value of 4.3 nM for binding to Aβ(1–40) fibrils (Fig. 6), this compound became our lead for further evaluations aimed at assessing how well the compound met the criteria shown in Table 1.[24]

Binding assays indicated that 6-OH-BTA-1 bound selectively with high affinity (K_i and K_d values in the range of 2–4 nM) to aggregated synthetic Aβ(1–40) and Aβ(1–42) fibrils and Aβ plaques in human AD brain tissues and with very poor affinity to NFTs.[25,26] Thus, a nonselective moderate-to-low-affinity pan-amyloid– binding fluorescent dye (thioflavin-T) was chemically modified to produce a neutral lipophilic PET radioligand with high binding affinity and high selectivity only for aggregated Aβ-containing fibrils and plaques. Additional in vivo brain uptake and clearance studies with [^{11}C]6-OH-BTA-1 in baboons demonstrated favorable pharmacokinetics of this compound with respect to the rapid clearance of radiotracer from healthy nonhuman primate brain.[24] We assessed the presence of radiolabeled metabolites in mouse brain after the injection of [^{11}C]6-OH-BTA-1 at times between 2 and 30 minutes after injection and determined that they were negligible.[24] It is interesting to note that other investigators have used rats to evaluate radiometabolites of [^{11}C]6-OH-BTA-1 in brain and have reported a relatively high level of radiolabeled metabolites in postmortem rat brain tissues.[27] We reported that rat appears to be unique in this regard, and that mice, baboons, and humans do not produce significant amounts of radiolabeled metabolites in their brains.[28] Attempts to use transgenic AD mice models that develop Aβ plaques to demonstrate specific binding met with failure initially,[25] and subsequent studies by other groups indicated that this failure was due to the relatively low B_{max} value in transgenic mouse models compared with human AD subjects and the subsequent necessity to use very-high-specific-activity [^{11}C]6-OH-BTA-1 for the transgenic mouse studies.[29,30] Thus, [^{11}C]6-OH-BTA-1 met all the acceptance criteria listed in Table 1, and human studies with this compound were then planned.

PET Imaging in Human Subjects With 6-OH-BTA-1

Because the toxicology and pharmacology of 6-OH-BTA-1 was not known, we were compelled by U.S. Food and Drug Administration (FDA) regulations in 2000 to conduct these studies in animals as part of an Investigational New Drug submission package. We sought and received National Institutes of Health/National Institute on Aging funding to conduct these studies at an estimated cost of approximately $200,000, and, while waiting for completion of the toxicologic studies, we contacted Bengt Långstrom, director of the Uppsala University PET Centre in Sweden, to discuss initiation of the first human PET study in Sweden using our Aβ radiotracer. We sought out the Uppsala PET Centre group because they had championed the microdosing concept.[31] Because of their very high specific activity and low cold mass, PET radiopharmaceuticals are typically given in "microdoses" of <10 μg, and subjects typically receive only 1 dose per year and seldom >4 doses per year. The microdosing concept holds that the preclinical safety evaluation of high-specific-activity PET radiopharmaceuticals should be tailored to how they are used and not judged by the same requirements originally developed by regulatory agencies interested in assuring the safety of therapeutic drugs typically given in milligram or gram quantities. Långstrom and colleagues led the efforts for these streamlined guidelines, and Swedish

regulatory authorities led the way in defining special pathways for microdosing toxicology. The FDA and other agencies have since adopted guidelines similar to those present in Sweden, as evidenced by the current exploratory Investigational New Drug mechanism for new PET and single-photon emission computed tomography imaging agents.[32]

When we first approached the Uppsala group in early 2001 regarding collaborative imaging studies, our lead Aβ imaging compound was not 6-OH-BTA-1, but instead was another compound we designated BTA-1.[23] BTA-1 is a close structural analog of 6-OH-BTA-1 and differs only by the presence of a 6-position H atom rather than the 6-OH group. Långstrom's group designated BTA-1 as "Pittsburgh Compound A" or PiA (the first compound sent to them by our group) in keeping with the tradition at Uppsala of naming compounds by a 3 letter designation.[33] As we conducted additional preclinical evaluations, we realized that 6-OH-BTA-1 was superior to BTA-1 and chose it as our lead compound, based primarily on its very good clearance rate from normal brain in rodents (Fig. 7) as well as in nonhuman primates.[24] The Uppsala group renamed 6-OH-BTA-1 "Pittsburgh Compound B" or PiB.[34]

By January of 2002, the necessary preliminary toxicologic studies and animal physiological studies with PiB were completed to satisfy the microdosing requirements at the Uppsala PET Centre, and the first subject for human PiB studies had been identified and evaluated by Agneta Nordberg. The first human study with PiB was conducted on February 14, 2002, in a relatively young woman whose memory problems had forced her to stop working as a health care professional.[35] From the first images sent to us from Uppsala (Fig. 8), it was immediately clear that the pattern of PiB retention matched the expected regional distribution of Aβ deposits previously reported from many postmortem studies.[36–38] A few weeks later, a negative PiB study in the first cognitively normal subject was conducted and demonstrated the rapid clearance of radiotracer from the same regions of brain that had retained PiB in the first study. A few months later, the preliminary findings from the first 9 AD subjects and 2 elderly and 3 young cognitively normal control subjects were presented at the "Hot Topics" session of the International Conference on Alzheimer's Disease in Stockholm on July 24, 2002, by Engler et al[39] of the Uppsala PET Centre team. The first peer-reviewed article describing this work[34] was published in early 2004, and since that time, >300 manuscripts describing PiB in Aβ studies have been reported.

The woman who provided that first human PiB PET image on Valentine's Day 2002 died in late 2007, and an autopsy confirmed what was suspected in 2002 when the first PiB image was viewed; PiB retention reflected the distribution of Aβ deposits in the brain.[35] This has now been confirmed by several correlative autopsy studies in other patients.[26,40,41] PiB scans are now performed in >60 research centers around the world, and we estimate that more than 10,000 investigational PiB PET scans have been performed. Conditions such as normal aging,[42–45] mild cognitive impairment[46–51] (MCI), AD,[52–55] early-onset familial AD,[56–59] and non-AD dementias[60–66] have been studied with PiB PET. Several current anti-amyloid drug trials have included a PiB component to assess the efficacy of the drug on the Aβ target.[67,68] This will be an important role of amyloid plaque imaging: facilitating the development of effective disease-modifying therapies. The finding that approximately 60% of MCI patients have levels of PiB retention similar to that seen in AD,[69,70] coupled with the finding that approximately 25% of cognitively normal elderly people in their 70s have measurable PiB retention,[71] suggests that one will need to look in asymptomatic people to find the earliest stages of AD pathology.[72] It may be that we have to identify and treat people at this early stage to achieve substantial disease-modifying effects. Our hope is that the benefit of PiB will ultimately be seen best in the development of new effective disease-modifying drugs along with the identification of the people who can best benefit from these drugs even before the first symptoms of AD become clinically apparent.

^{18}F-Labeled Aβ Imaging Agents

Work over the past 6 years at many institutions has focused on developing ^{18}F-labeled PET radiotracers for more wide-spread availability and routine clinical usefulness than ^{11}C-labeled PiB. At Pittsburgh, we synthesized and evaluated several hundred fluorinated compounds as potential ^{18}F-labeled Aβ imaging agents. These efforts led to the development of an ^{18}F-labeled PiB derivative, 3'-F-PiB (Fig. 9), and this compound is also known as GE-067 and flutemetamol.[73–75] Chemists at the University of Pennsylvania and Avid Radiopharmaceuticals (Philadelphia, PA) explored fluorinated analogs of the stilbene [^{11}C]SB-13[76] (Fig. 9) and derived AV-1 (also known as BAY 94–9172 and florbetaben)[77–79] and AV-45 (also known as florbetapir and Amyvid™ (Eli Lilly and Company, Indianapolis, IN)).[80–83] Chemists at AstraZeneca (Södertälje, Sweden) explored structural analogs of PiB, and developed AZD4694 (Fig. 9), the in vivo properties of which in human subjects have recently been reported.[84] From a chemical homology viewpoint, all of these derivatives are related to the PiB framework as shown in Fig. 10. From a binding perspective, all the compounds shown in Fig. 10 appear to bind selectively with high affinity to aggregated (fibrillar) Aβ and do not bind well to aggregated tau forms such as NFTs. From an in vivo imaging perspective, all the compounds have been shown to readily distinguish subjects with high brain Aβ plaque loads from those with little or no significant Aβ plaque loads. The relative sensitivities and specificities of the compounds for detecting and quantifying different levels of Aβ loads in human subjects remain an area of active investigation.[74,85–87]

Clinical Use of ^{18}F-Labeled Aβ Imaging Agents

Amyvid™ was approved by the FDA for human clinical Aβ imaging in April 2012,[88] and other ^{18}F-labeled agents (flutemetamol, florbetaben, and AZD4694) are currently in phase II or phase III FDA clinical trials in the United States. We believe that the greatest utility of the new ^{18}F-labeled Aβ imaging agents will be similar to that we envisioned for PiB: these agents likely will prove useful in identifying efficacious anti-amyloid therapies that can prevent or delay AD, as well as identifying those subjects who likely will benefit from these therapies long before the clinical diagnosis of probable AD.[89]

The development of PiB as a highly potent and selective PET radioligand for fibrillar Aβ was in good part serendipitous. It resulted from a chemical change in the pan-amyloid fluorescent dye thioflavin-T aimed at increasing brain penetration of neutral BTA derivatives, but that structural change also produced derivatives with both high affinity and selectivity for fibrillar Aβ. This outcome was highly fortuitous for several reasons: (1) interpretation of the specific binding of PiB in human brain is unambiguous, as it binds to only 1 amyloid target; and (2) dysregulation of Aβ is believed to be the first biomarker altered in the course of AD, making a selective imaging agent for Aβ important and useful for early disease detection.[90–92] Other biomarkers that more fully reflect AD progression and disease stage, such as NFTs, regional hypometabolism, and cortical gray matter atrophy, are believed to be altered after (ie, downstream of) Aβ dysregulation. Recently, great progress has been realized in the use of [^{18}F]fluorodeoxyglucose (FDG) and structural magnetic resonance imaging to assess regional brain hypometabolism and cortical atrophy in MCI and AD. In contrast, progress in developing a selective PET radioligand to quantify NFTs in living human brain has lagged, but recent advances are encouraging. [93,94] The combined use of selective Aβ plaque and NFT PET agents, along with FDG and structural magnetic resonance imaging, will likely provide even greater insights into the pathophysiology of AD at all stages of the disease process: from cognitively normal elderly subjects to MCI subjects to AD patients. It is hoped that these imaging insights will assist in the development of effective disease-modifying treatments for AD, and that subjects very

early in the course of the disease process will be identified and will benefit most greatly from these future therapeutic treatments.

Acknowledgments

The authors thank Steven T. DeKosky, MD, Julie C. Price, PhD, and Milos D. Ikonomovic, MD, for their extensive and critical contributions to the development of the Aβ imaging program in Pittsburgh. They also thank members of the original chemistry team that developed PiB: Daniel Holt, Guofeng Huang, PhD, Manik Debnath, and Li Shao, PhD, for their contributions to this development program. The expert and caring work of the clinical teams at the University of Pittsburgh Alzheimer's Disease Research Center and University of Pittsburgh Medical Center PET Facility are greatly appreciated. Funding support for portions of the development program was provided by grants from the National Institutes of Health (R01 AG018402, P50 AG005133, K02 AG001039, R01 AG020226, R01 MH070729, K01 MH001976, R37 AG025516, P01 AG025204), the Alzheimer's Association (TLL-01-3381), GE Healthcare, and the US Department of Energy (DE-FD02-03 ER63590). These funding agencies had no role in the design or interpretation of results or preparation of this manuscript.

References

1. Klunk WE, Debnath ML, Pettegrew JW. Development of small molecule probes for the beta-amyloid protein of Alzheimer's disease. Neurobiol Aging. 1994; 15:691–698. [PubMed: 7891823]
2. Mathis CA, Mahmood K, Debnath ML, et al. Synthesis of a lipophilic radioiodinated ligand with high affinity to amyloid protein in Alzheimer's disease brain tissue. J Label Comp Radiopharm. 1997; 40:94–95. (abstract).
3. Mathis CA, Wang Y, Klunk WE. Imaging beta-amyloid plaques and neurofibrillary tangles in the aging human brain. Curr Pharm Des. 2004; 10:1469–1492. [PubMed: 15134570]
4. Alzheimer A. Uber eine eigenartige erkrankung der hirnrinde [About a peculiar disease of the cerebral cortex] [in German]. Allgemeine Zeitschrift fur Psychiatrie und Pyschisch-Gerichtlich Medizin. 1907; 64:146–148.
5. Klunk WE, Debnath ML, Pettegrew JW. Chrysamine-G binding to Alzheimer and control brain: Autopsy study of a new amyloid probe. Neurobiol Aging. 1995; 16:541–548. [PubMed: 8544903]
6. Dishino DD, Welch MJ, Kilbourn MR, et al. Relationship between lipophilicity and brain extraction of C-11-labeled radiopharmaceuticals. J Nucl Med. 1983; 24:1030–1038. [PubMed: 6605416]
7. Waterhouse RN. Determination of lipophilicity and its use as a predictor of blood-brain barrier penetration of molecular imaging agents. Mol Imaging Biol. 2003; 5:376–389. [PubMed: 14667492]
8. Styren SD, Hamilton RL, Styren GC, et al. X-34, a fluorescent derivative of Congo red: A novel histochemical stain for Alzheimer's disease pathology. J Histochem Cytochem. 2000; 48:1223–1232. [PubMed: 10950879]
9. Klunk WE, Jacob RF, Mason RP. Quantifying amyloid beta-peptide (Abeta) aggregation using the Congo red-Abeta (CR-Abeta) spectro-photometric assay. Anal Biochem. 1999; 266:66–76. [PubMed: 9887214]
10. Farde L, Hall H, Ehrin E, et al. Quantitative analysis of D2 dopamine receptor binding in the living human brain by PET. Science. 1986; 231:258–261. [PubMed: 2867601]
11. Hsiao K, Chapman P, Nilsen S, et al. Correlative memory deficits, Aβ elevation, and amyloid plaques in transgenic mice. Science. 1996; 274:99–103. [PubMed: 8810256]
12. Klunk WE, Debnath ML, Koros AM, et al. Chrysamine-G, a lipophilic analogue of Congo red, inhibits A beta-induced toxicity in PC12 cells. Life Sci. 1998; 63:1807–1814. [PubMed: 9820124]
13. Ishii K, Klunk WE, Arawaka S, et al. Chrysamine G and its derivative reduce amyloid beta-induced neurotoxicity in mice. Neurosci Lett. 2002; 333:5–8. [PubMed: 12401547]
14. Ikonomovic MD, Abrahamson EE, Isanski BA, et al. X-34 labeling of abnormal protein aggregates during the progression of Alzheimer's disease. Methods Enzymol. 2006; 412:123–144. [PubMed: 17046656]
15. Klunk WE, Bacskai BJ, Mathis CA, et al. Imaging Abeta plaques in living transgenic mice with multiphoton microscopy and methoxy-X04, a systemically administered Congo red derivative. J Neuropathol Exp Neurol. 2002; 61:797–805. [PubMed: 12230326]

16. Brendza RP, Bacskai BJ, Cirrito JR, et al. Anti-Abeta antibody treatment promotes the rapid recovery of amyloid-associated neuritic dystrophy in PDAPP transgenic mice. J Clin Invest. 2005; 115:428–433. [PubMed: 15668737]
17. Meyer-Luehmann M, Spires-Jones TL, Prada C, et al. Rapid appearance and local toxicity of amyloid-beta plaques in a mouse model of Alzheimer's disease. Nature. 2008; 451:720–724. [PubMed: 18256671]
18. Burgold S, Bittner T, Dorostkar MM, et al. In vivo multiphoton imaging reveals gradual growth of newborn amyloid plaques over weeks. Acta Neuropathol. 2011; 121:327–335. [PubMed: 21136067]
19. Sadowski M, Pankiewicz J, Scholtzova H, et al. Targeting prion amyloid deposits in vivo. J Neuropathol Exp Neurol. 2004; 63:775–784. [PubMed: 15290902]
20. Skovronsky DM, Zhang B, Kung MP, et al. In vivo detection of amyloid plaques in a mouse model of Alzheimer's disease. Proc Natl Acad Sci USA. 2000; 97:7609–7614. [PubMed: 10861023]
21. Maezawa I, Hong HS, Liu R, et al. Congo red and thioflavin-T analogs detect Abeta oligomers. J Neurochem. 2008; 104:457–468. [PubMed: 17953662]
22. Klunk WE, Wang Y, Huang GF, et al. Uncharged thioflavin-T derivatives bind to amyloid-beta protein with high affinity and readily enter the brain. Life Sci. 2001; 200:1471–1484. [PubMed: 11554609]
23. Mathis CA, Bacskai BJ, Kajdasz ST, et al. A lipophilic thioflavin-T derivative for positron emission tomography (PET) imaging of amyloid in brain. Bioorg Med Chem Lett. 2002; 12:295–298. [PubMed: 11814781]
24. Mathis CA, Wang Y, Holt DP, et al. Synthesis and evaluation of 11C-labeled 6-substituted 2-arylbenzothiazoles as amyloid imaging agents. J Med Chem. 2003; 46:2740–2754. [PubMed: 12801237]
25. Klunk WE, Lopresti BJ, Ikonomovic MD, et al. Binding of the positron emission tomography tracer Pittsburgh compound-B reflects the amount of amyloid-beta in Alzheimer's disease brain but not in transgenic mouse brain. J Neurosci. 2005; 25:10598–10606. [PubMed: 16291932]
26. Ikonomovic MD, Klunk WE, Abrahamson EE, et al. Post-mortem correlates of in vivo PiB-PET amyloid imaging in a typical case of Alzheimer's disease. Brain. 2008; 131:1630–1645. [PubMed: 18339640]
27. Phelps ME, Barrio JR. Correlation of brain amyloid with "aerobic glycolysis": A question of assumptions? Proc Natl Acad Sci USA. 2010; 107:17459–17460. [PubMed: 20921385]
28. Mathis CA, Holt DP, Wang Y, et al. Species-dependent metabolism of the amyloid imaging agent [C-11]PIB. J Nucl Med. 2004; 45:114P. (abstract).
29. Maeda J, Ji B, Irie T, et al. Longitudinal, quantitative assessment of amyloid, neuroinflammation, and anti-amyloid treatment in a living mouse model of Alzheimer's disease enabled by positron emission tomography. J Neurosci. 2007; 27:10957–10968. [PubMed: 17928437]
30. Manook A, Yousefi BH, Willuweit A, et al. Small-animal PET imaging of amyloid-beta plaques with [11C]PiB and its multi-modal validation in an APP/PS1 mouse model of Alzheimer's disease. PLoS One. 2012; 7:e31310. [PubMed: 22427802]
31. Bergström M, Grahnén A, Långström B. Positron emission tomography microdosing: A new concept with application in tracer and early clinical drug development. Eur J Clin Pharmacol. 2003; 59:357–366. [PubMed: 12937873]
32. Mills G. The exploratory IND. J Nucl Med. 2008; 49:45N–47N.
33. Klunk WE, Mathis CA. Whatever happened to Pittsburgh compound-A? Alzheimer Dis Assoc Disord. 2008; 22:198–203. [PubMed: 18769172]
34. Klunk WE, Engler H, Nordberg A, et al. Imaging brain amyloid in Alzheimer's disease with Pittsburgh Compound-B. Ann Neurol. 2004; 55:306–319. [PubMed: 14991808]
35. Kadir A, Marutle A, Gonzalez D, et al. Positron emission tomography imaging and clinical progression in relation to molecular pathology in the first Pittsburgh Compound B positron emission tomography patient with Alzheimer's disease. Brain. 2011; 134:301–317. [PubMed: 21149866]

36. Arnold SE, Hyman BT, Flory J, et al. The topographical and neuroanatomical distribution of neurofibrillary tangles and neuritic plaques in the cerebral cortex of patients with Alzheimer's disease. Cereb Cortex. 1991; 1:103–116. [PubMed: 1822725]
37. Braak H, Braak E. Frequency of stages of Alzheimer-related lesions in different age categories. Neurobiol Aging. 1997; 18:351–357. [PubMed: 9330961]
38. Thal DR, Rüb U, Schultz C, et al. Sequence of Abeta-protein deposition in the human medial temporal lobe. J Neuropathol Exp Neurol. 2000; 59:733–748. [PubMed: 10952063]
39. Engler H, Blomqvist G, Bergstrom M, et al. First human study with a benzothiazole amyloid-imaging agent in Alzheimer's disease and control subjects. Neurobiol Aging. 2002; 23(suppl): 1568. (abstract).
40. Bacskai BJ, Frosch MP, Freeman SH, et al. Molecular imaging with Pittsburgh compound B confirmed at autopsy: A case report. Arch Neurol. 2007; 64:431–434. [PubMed: 17353389]
41. Ikonomovic MD, Abrahamson EE, Price JC, et al. Early AD pathology in a [C-11]PiB-negative case: A PiB-amyloid imaging, biochemical, and immunohistochemical study. Acta Neuropathol. 2012; 12:433–447. [PubMed: 22271153]
42. Mintun MA, Larossa GN, Sheline YI, et al. [^{11}C]PIB in a nondemented population: Potential antecedent marker of Alzheimer disease. Neurology. 2006; 67:446–452. [PubMed: 16894106]
43. Pike KE, Savage G, Villemagne VL, et al. β-amyloid imaging and memory in non-demented individuals: Evidence for preclinical Alzheimer's disease. Brain. 2007; 130:2837–2844. [PubMed: 17928318]
44. Aizenstein HJ, Nebes RD, Saxton JA, et al. Frequent amyloid deposition without significant cognitive impairment among the elderly. Arch Neurol. 2008; 65:1509–1517. [PubMed: 19001171]
45. Pike KE, Ellis KA, Villemagne VL, et al. Cognition and beta-amyloid in preclinical Alzheimer's disease: Data from the AIBL study. Neuropsychologia. 2011; 49:2384–2390. [PubMed: 21529702]
46. Forsberg A, Engler H, Almkvist O, et al. PET imaging of amyloid deposition in patients with mild cognitive impairment. Neurobiol Aging. 2008; 29:1456–1465. [PubMed: 17499392]
47. Kemppainen NM, Aalto S, Wilson IA, et al. PET amyloid ligand [11C]PIB uptake is increased in mild cognitive impairment. Neurology. 2007; 68:1603–1606. [PubMed: 17485647]
48. Wolk DA, Price JC, Saxton JA, et al. Amyloid imaging in mild cognitive impairment subtypes. Ann Neurol. 2009; 65:557–568. [PubMed: 19475670]
49. Okello A, Koivunen J, Edison P, et al. Conversion of amyloid positive and negative MCI to AD over 3 years: An 11C-PIB PET study. Neurology. 2009; 73:754–760. [PubMed: 19587325]
50. Villemagne VL, Pike KE, Chételat G, et al. Longitudinal assessment of Aβ and cognition in aging and Alzheimer disease. Ann Neurol. 2011; 69:181–192. [PubMed: 21280088]
51. Koivunen J, Scheinin N, Virta JR, et al. Amyloid PET imaging in patients with mild cognitive impairment: A 2-year follow-up study. Neurology. 2011; 76:1085–1090. [PubMed: 21325653]
52. Rowe CC, Ng S, Ackermann U, et al. Imaging beta-amyloid burden in aging and dementia. Neurology. 2007; 68:1718–1725. [PubMed: 17502554]
53. Jack CR Jr, Lowe VJ, Senjem ML, et al. 11C PiB and structural MRI provide complementary information in imaging of Alzheimer's disease and amnestic mild cognitive impairment. Brain. 2008; 131:665–680. [PubMed: 18263627]
54. Fodero-Tavoletti MT, Cappai R, McLean CA, et al. Amyloid imaging in Alzheimer's disease and other dementias. Brain Imaging Behav. 2009; 3:246–261. [PubMed: 22005989]
55. Kadir A, Almkvist O, Forsberg A, et al. Dynamic changes in PET amyloid and FDG imaging at different stages of Alzheimer's disease. Neurobiol Aging. 2012; 33:198e1–198e14. [PubMed: 20688420]
56. Theuns J, Marjaux E, Vandenbulcke M, et al. Alzheimer dementia caused by a novel mutation located in the APP C-terminal intracytosolic fragment. Hum Mutat. 2006; 27:888–896. [PubMed: 16917905]
57. Klunk WE, Price JC, Mathis CA, et al. Amyloid deposition begins in the striatum of presenilin-1 mutation carriers from two unrelated pedigrees. J Neurosci. 2007; 27:6174–6184. [PubMed: 17553989]

58. Remes AM, Laru L, Tuominen H, et al. Carbon 11-labeled Pittsburgh Compound B positron emission tomographic amyloid imaging in patients with APP locus duplication. Arch Neurol. 2008; 65:540–544. [PubMed: 18413480]
59. Villemagne VL, Pike K, Pejoska S, et al. 11C-PiB PET ABri imaging in Worster-Drought syndrome (familial British dementia): A case report. J Alzheimers Dis. 2010; 19:423–428. [PubMed: 20110591]
60. Johansson A, Savitcheva I, Forsberg A, et al. [(11)C]-PIB imaging in patients with Parkinson's disease: Preliminary results. Parkinsonism Relat Disord. 2008; 14:345–347. [PubMed: 17855149]
61. Rabinovici GD, Furst AJ, O'Neil JP, et al. ^{11}C-PIB PET imaging in Alzheimer disease and frontotemporal lobar degeneration. Neurology. 2007; 68:1205–1212. [PubMed: 17420404]
62. Drzezga A, Grimmer T, Henriksen G, et al. Imaging of amyloid plaques and cerebral glucose metabolism in semantic dementia and Alzheimer's disease. Neuroimage. 2008; 39:619–633. [PubMed: 17962045]
63. Maetzler W, Reimold M, Liepelt I, et al. [11C]PIB binding in Parkinson's disease dementia. Neuroimage. 2008; 39:1027–1033. [PubMed: 18035558]
64. Rabinovici GD, Rosen HJ, Alkalay A, et al. Amyloid vs FDG-PET in the differential diagnosis of AD and FTLD. Neurology. 2011; 77:2034–2042. [PubMed: 22131541]
65. Leyton CE, Villemagne VL, Savage S, et al. Subtypes of progressive aphasia: Application of the International Consensus Criteria and validation using β-amyloid imaging. Brain. 2011; 134:3030–3043. [PubMed: 21908392]
66. Caso F, Gesierich B, Henry M, et al. Nonfluent/agrammatic PPA with in-vivo cortical amyloidosis and Pick's disease pathology. Behav Neurol. 2012 Apr 24. [Epub ahead of print].
67. Rinne JO, Brooks DJ, Rossor MN, et al. 11C-PiB PET assessment of change in fibrillar amyloid-beta load in patients with Alzheimer's disease treated with bapineuzumab: A phase 2, double-blind, placebo-controlled, ascending-dose study. Lancet Neurol. 2010; 9:363–372. [PubMed: 20189881]
68. Ostrowitzki S, Deptula D, Thurfjell L, et al. Mechanism of amyloid removal in patients with Alzheimer disease treated with gantenerumab. Arch Neurol. 2012; 69:198–207. [PubMed: 21987394]
69. Rowe CC, Ellis KA, Rimajova M, et al. Amyloid imaging results from the Australian Imaging, Biomarkers and Lifestyle (AIBL) study of aging. Neurobiol Aging. 2010; 31:1275–1283. [PubMed: 20472326]
70. Jagust WJ, Bandy D, Chen K, et al. The Alzheimer's Disease Neuroimaging Initiative positron emission tomography core. Alzheimers Dement. 2010; 6:221–229. [PubMed: 20451870]
71. Klunk WE. Amyloid imaging as a biomarker for cerebral β-amyloidosis and risk prediction for Alzheimer dementia. Neurobiol Aging. 2011; 32(suppl 1):S20–S36. [PubMed: 22078170]
72. Sperling RA, Aisen PS, Beckett LA, et al. Toward defining the preclinical stages of Alzheimer's disease: Recommendations from the National Institute on Aging-Alzheimer's Association workgroups on diagnostic guidelines for Alzheimer's disease. Alzheimers Dement. 2011; 7:280–292. [PubMed: 21514248]
73. Mathis CA, Lopresti B, Mason N, et al. Comparison of the amyloid imaging agents [F-18]3'-F–PIB and [C-11]PIB in Alzheimer's disease and control subjects. J Nucl Med. 2007; 48:56P. (abstract). [PubMed: 17204699]
74. Vandenberghe R, Van Laere K, Ivanoiu A, et al. 18F-flutemetamol amyloid imaging in Alzheimer disease and mild cognitive impairment: A phase 2 trial. Ann Neurol. 2010; 68:319–329. [PubMed: 20687209]
75. Thurfjell L, Lötjönen J, Lundqvist R, et al. Combination of biomarkers: PET [^{18}F]flutemetamol imaging and structural MRI in dementia and mild cognitive impairment. Neurodegener Dis. 2012; 10:246–249. [PubMed: 22301718]
76. Verhoeff NP, Wilson AA, Takeshita S, et al. In-vivo imaging of Alzheimer disease beta-amyloid with [^{11}C]SB-13 PET. Am J Geriatr Psychiatry. 2004; 12:584–595. [PubMed: 15545326]
77. Rowe CC, Ackerman U, Browne W, et al. Imaging of amyloid beta in Alzheimer's disease with 18F-BAY94-9172, a novel PET tracer: Proof of mechanism. Lancet Neurol. 2008; 7:129–135. [PubMed: 18191617]

78. Barthel H, Luthardt J, Becker G, et al. Individualized quantification of brain β-amyloid burden: Results of a proof of mechanism phase 0 florbetaben PET trial in patients with Alzheimer's disease and healthy controls. Eur J Nucl Med Mol Imaging. 2011; 38:1702–1714. [PubMed: 21547601]
79. Barthel H, Gertz HJ, Dresel S, et al. Cerebral amyloid-β PET with florbetaben (18F) in patients with Alzheimer's disease and healthy controls: A multicentre phase 2 diagnostic study. Lancet Neurol. 2011; 10:424–435. [PubMed: 21481640]
80. Wong DF, Rosenberg PB, Zhou Y, et al. In vivo imaging of amyloid deposition in Alzheimer disease using the radioligand 18F-AV-45 (florbetapir [corrected] F 18). J Nucl Med. 2010; 51:913–920. [PubMed: 20501908]
81. Choi SR, Schneider JA, Bennett DA, et al. Correlation of amyloid PET ligand florbetapir F 18 binding with Aβ aggregation and neuritic plaque deposition in postmortem brain tissue. Alzheimer Dis Assoc Disord. 2012; 26:8–16. [PubMed: 22354138]
82. Clark CM, Pontecorvo MJ, Beach TG, et al. Cerebral PET with florbetapir compared with neuropathology at autopsy for detection of neuritic amyloid-β plaques: A prospective cohort study. Lancet Neurol. 2012; 11:669–678. [PubMed: 22749065]
83. Joshi AD, Pontecorvo MJ, Clark CM, et al. Performance characteristics of amyloid PET with florbetapir F 18 in patients with Alzheimer's disease and cognitively normal subjects. J Nucl Med. 2012; 53:378–384. [PubMed: 22331215]
84. Cselényi Z, Jönhagen ME, Forsberg A, et al. Clinical validation of 18F-AZD4694, an amyloid-β-specific PET radioligand. J Nucl Med. 2012; 53:415–424. [PubMed: 22323782]
85. Jagust WJ. Amyloid imaging: Liberal or conservative? Let the data decide. Arch Neurol. 2011; 68:1377–1378. (editorial). [PubMed: 21747005]
86. Villemagne VL, Mulligan RS, Pejoska S, et al. Comparison of 11C-PiB and 18F-florbetaben for Aβ imaging in ageing and Alzheimer's disease. Eur J Nucl Med Mol Imaging. 2012; 39:983–989. [PubMed: 22398958]
87. Hsiao IT, Huang CC, Hsieh CJ, et al. Correlation of early-phase 18F-florbetapir (AV-45/Amyvid) PET images to FDG images: Preliminary studies. Eur J Nucl Med Mol Imaging. 2012; 39:613–620. [PubMed: 22270508]
88. FDA approves 18F-florbetapir PET agent. J Nucl Med. 2012; 53:15N. (editorial).
89. Sperling RA, Johnson KA. Dementia: New criteria but no new treatments. Lancet Neurol. 2012; 11:4–5. (editorial). [PubMed: 22172609]
90. Jack CR Jr, Knopman DS, Jagust WJ, et al. Hypothetical model of dynamic biomarkers of the Alzheimer's pathological cascade. Lancet Neurol. 2010; 9:119–128. [PubMed: 20083042]
91. Jack CR Jr, Vemuri P, Wiste HJ, et al. Evidence for ordering of Alzheimer disease biomarkers. Arch Neurol. 2011; 68:1526–1535. [PubMed: 21825215]
92. Sperling RA, Jack CR Jr, Aisen PS. Testing the right target and right drug at the right stage. Sci Transl Med. 2011; 3:111. (editorial).
93. Fodero-Tavoletti MT, Okamura N, Furumoto S, et al. 18F-THK523: A novel in vivo tau imaging ligand for Alzheimer's disease. Brain. 2011; 134:1089–1100. [PubMed: 21436112]
94. Zhang W, Arteaga J, Cashion DK, et al. A highly selective and specific PET tracer for imaging of tau pathologies. J Alzheimers Dis. 2012 Jun 8. [Epub ahead of print].

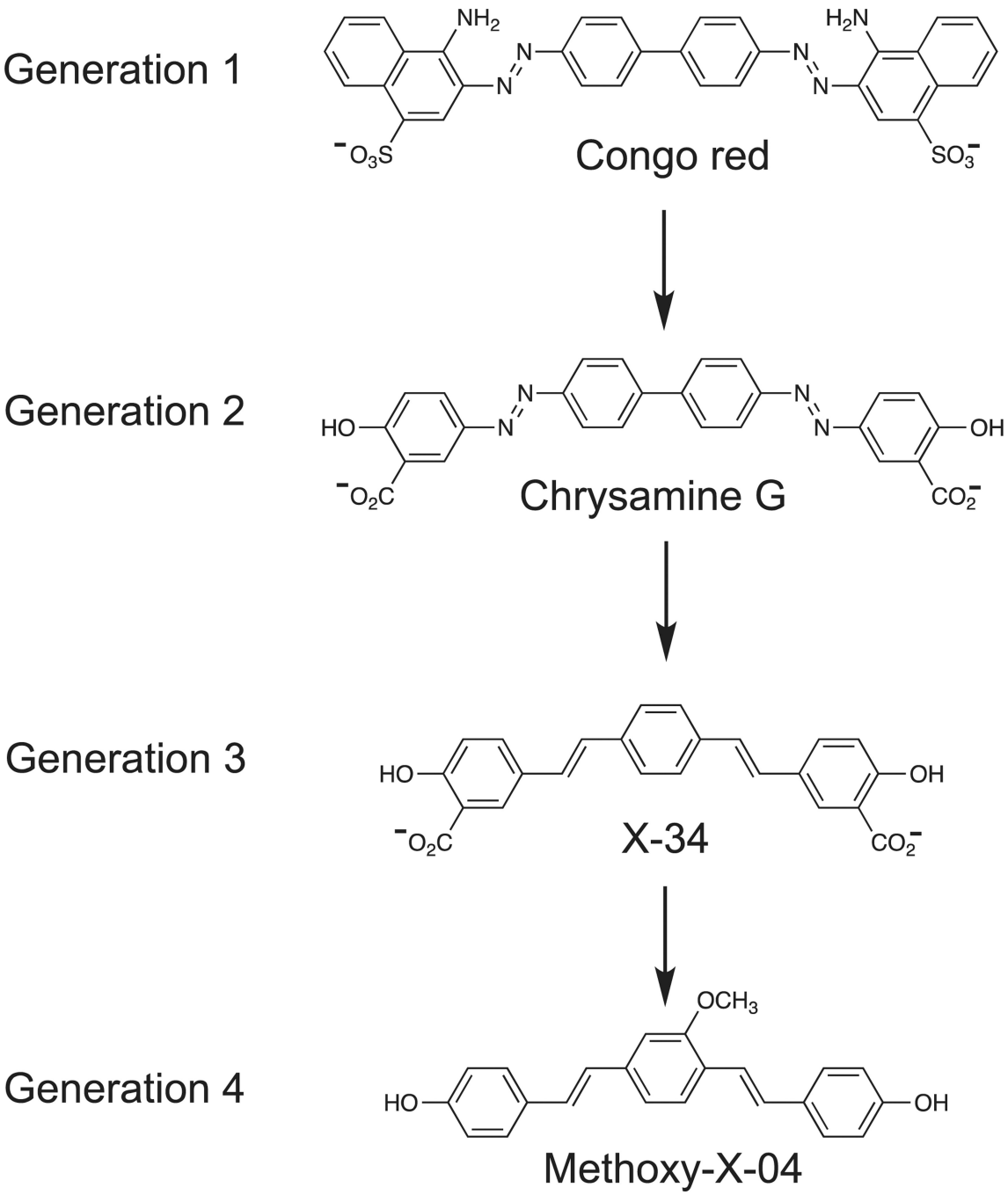

Figure 1.
Four generations of Congo Red and derivatives evaluated as potential PET amyloid imaging agents.

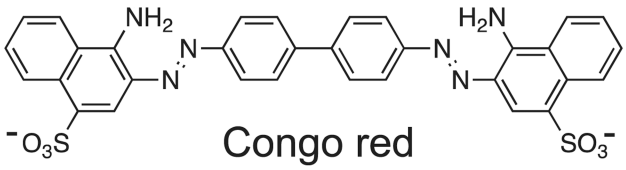

Congo red

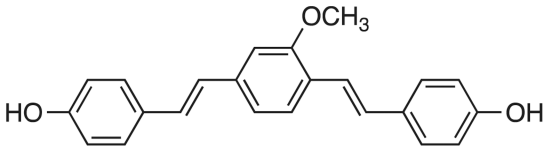

Methoxy-X-04

Aβ Peptides and Aβ Antibodies

Tau Peptides and Tau Antibodies

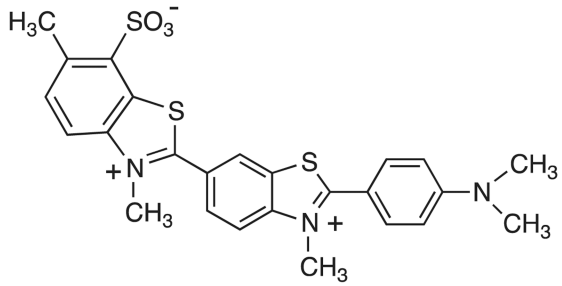

Thioflavin-S

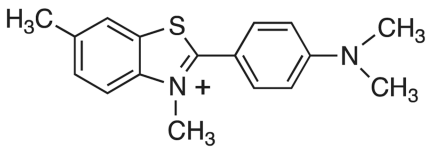

Thioflavin-T

Figure 2.
Potential amyloid-binding pharmacophores.

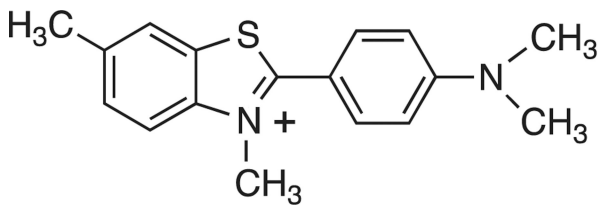

Thioflavin-T

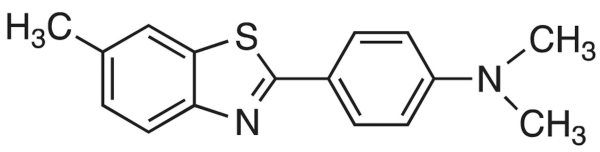

6-Me-BTA-2

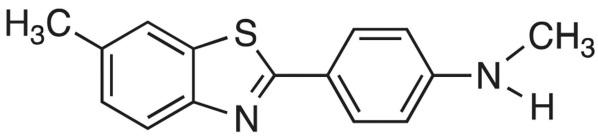

6-Me-BTA-1

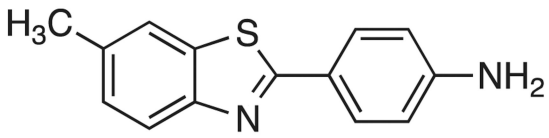

6-Me-BTA-0

Figure 3.
Structures of 3 neutral thioflavin-T analogs.

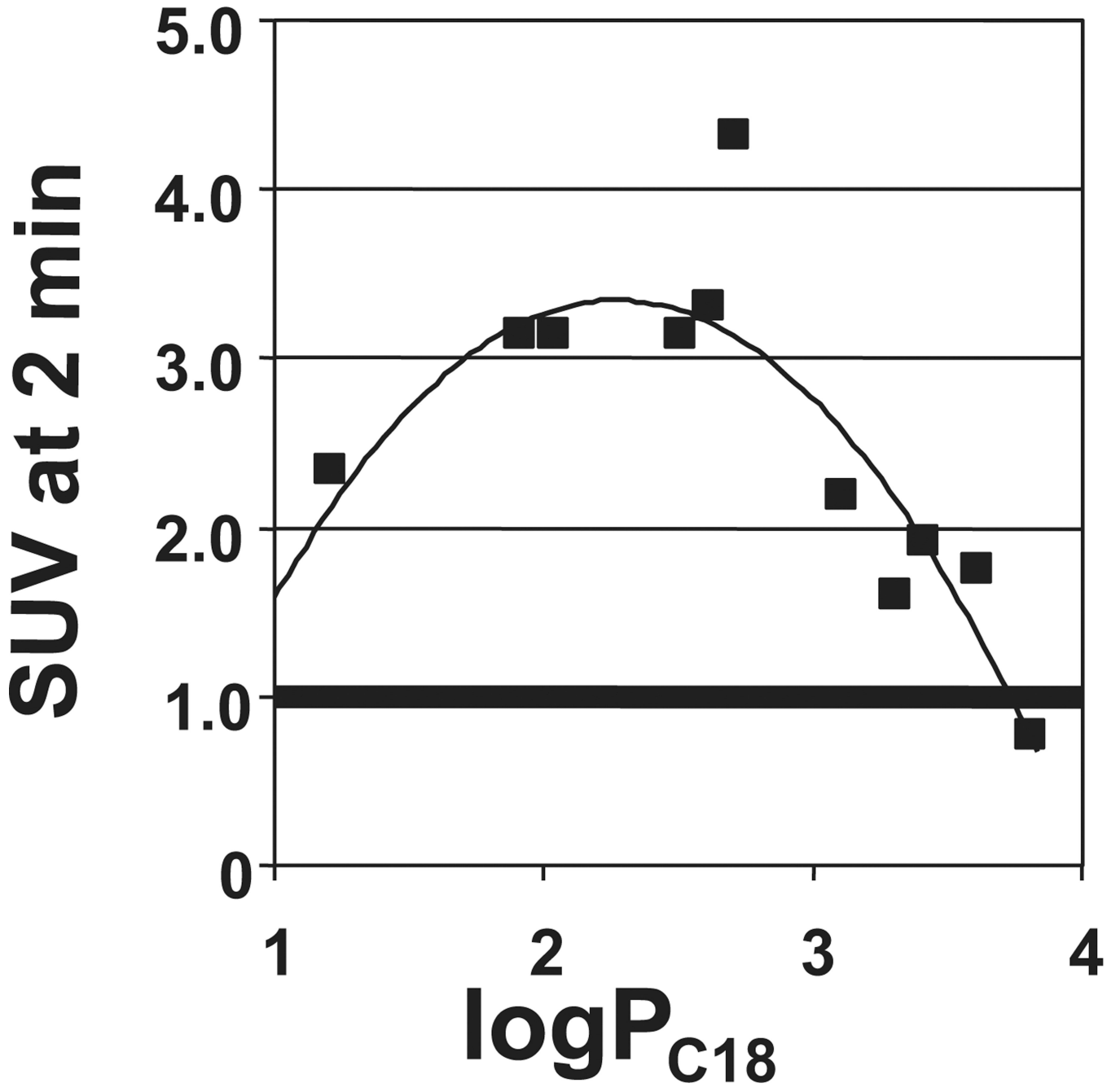

Figure 4.

Relationship between normal mouse brain concentration (SUV is the standardized uptake value) for 11 ^{11}C-labeled BTA compounds 2 minutes after iv injection and the lipophilicity of the compounds as assessed by the logarithm of the reverse-phase HPLC–derived partition coefficient ($\log P_{C18}$), which is proportional to the logD value of the derivatives.

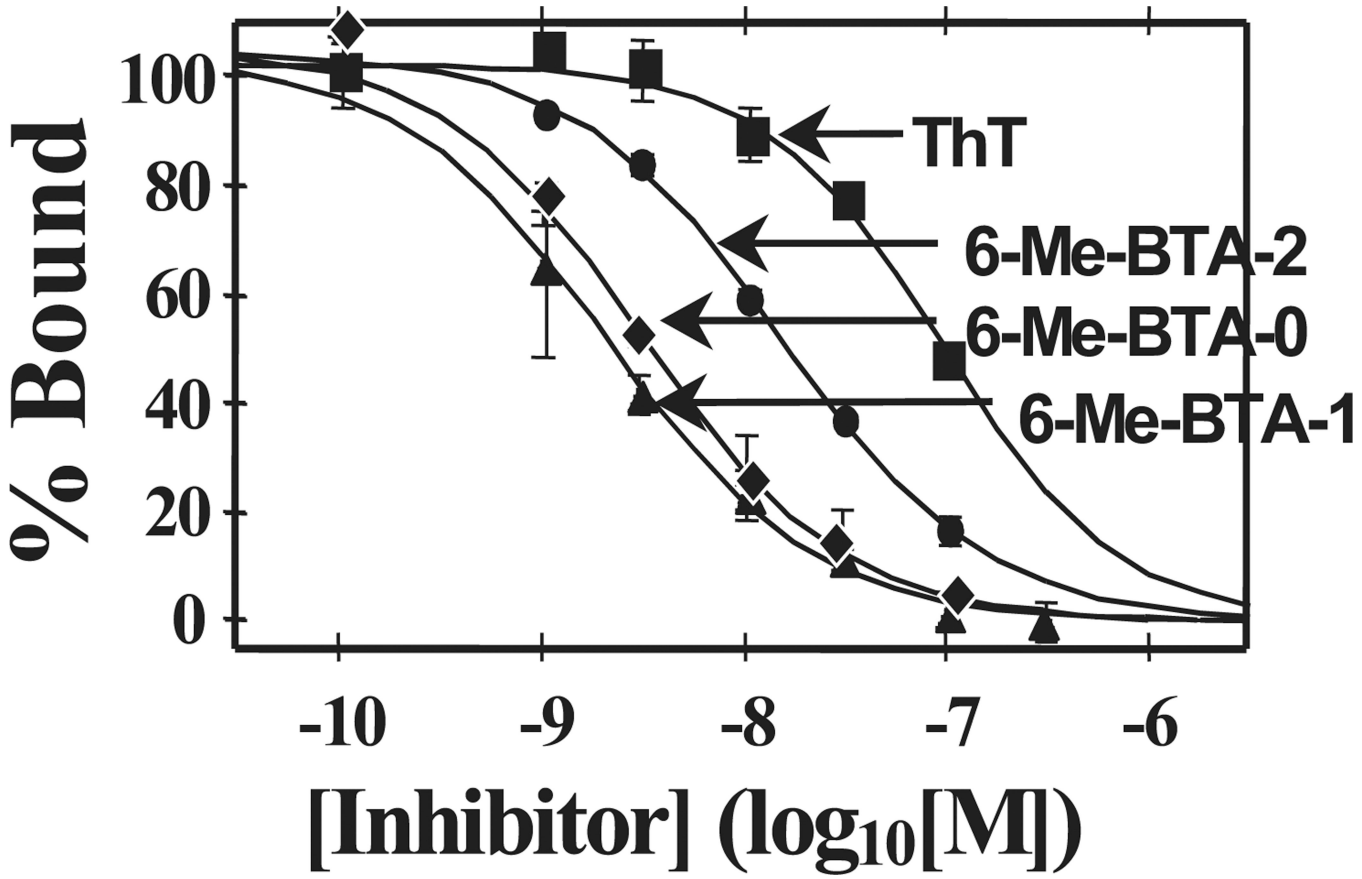

Figure 5.
Binding affinity of 3 neutral BTA compounds, the structures of which are shown in Figure 3, relative to thioflavin-T (ThT) for synthetic Aβ(1–40) fibrils.

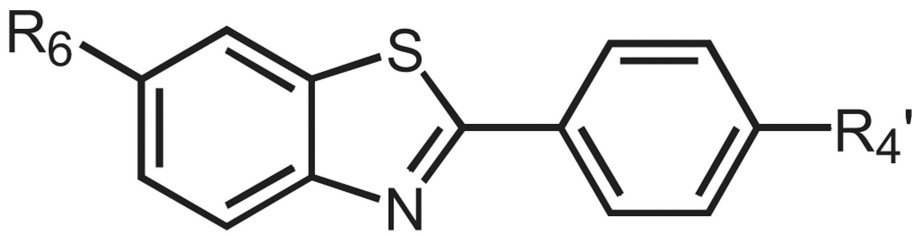

Affinity (K_i, nM) for Aβ(1-40) fibrils

R_6	R_4' = NH_2	R_4' = $NHCH_3$	R_4' = $N(CH_3)_2$
CH_3	9.5	10	64
H	37	10	4.0
HO	46	4.3	4.4
CH_3O	7.0	4.9	1.9

Figure 6.
Structure–affinity values for representative BTA analogs. The K_i values were determined using [^{3}H]BTA-1 (R_6 = H, R4' = $NHCH_3$) as the radioligand and synthetic Aβ(1–40) fibrils as the binding site protein.

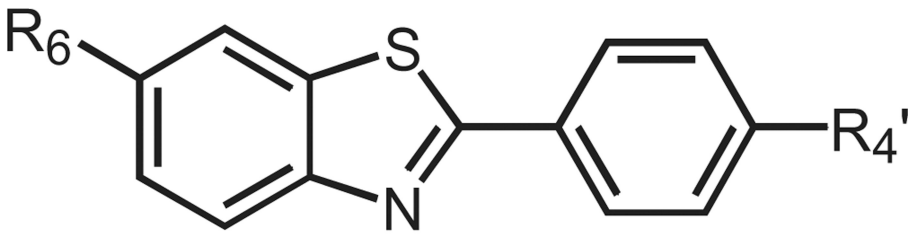

Ratio of 2':30' brain uptake values

R_6	R_4' = NH_2	$NHCH_3$	$N(CH_3)_2$
CH_3	-	2.7	0.5
H	-	7.6	2.5
HO	-	11	3.0
CH_3O	3.8	3.2	1.1

Figure 7.
Structure–clearance values for representative BTA analogs from normal mice brain. Values are the ratio of the %ID/g concentrations in mouse brain at 2 minutes after injection to the %ID/g concentrations at 30 minutes after injection.

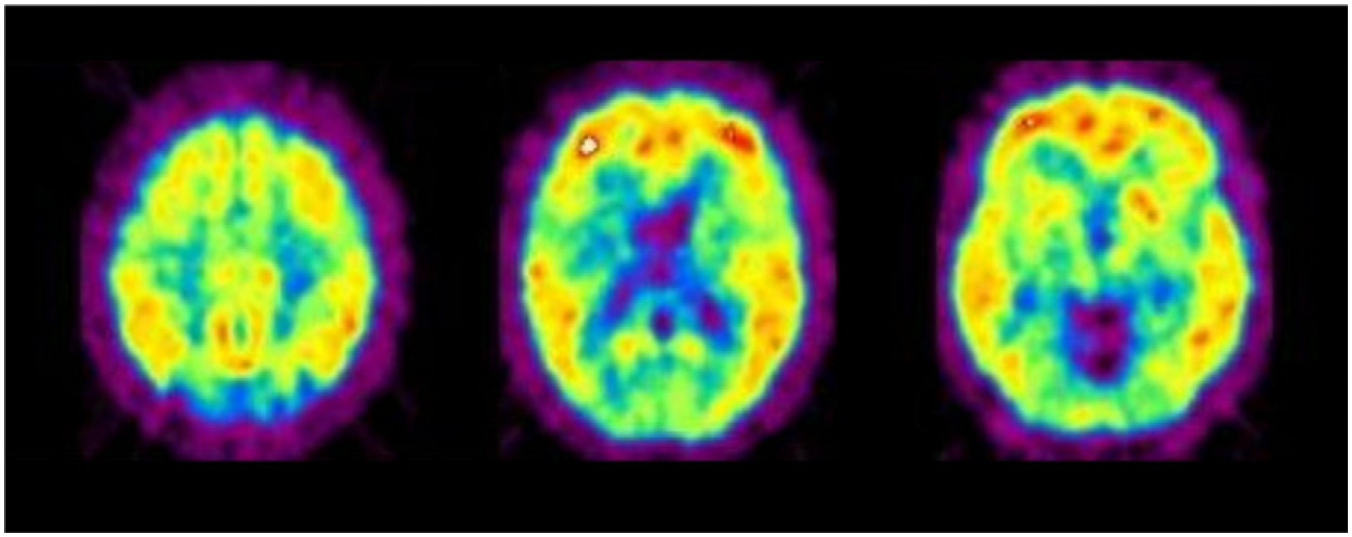

Figure 8.
First human PiB PET images obtained on February 14, 2002, by Bengt Långström and colleagues at the Uppsala University PET Centre from the first volunteer (mild AD, MMSE = 25; Reprinted with permission from Klunk and Mathis[34]).

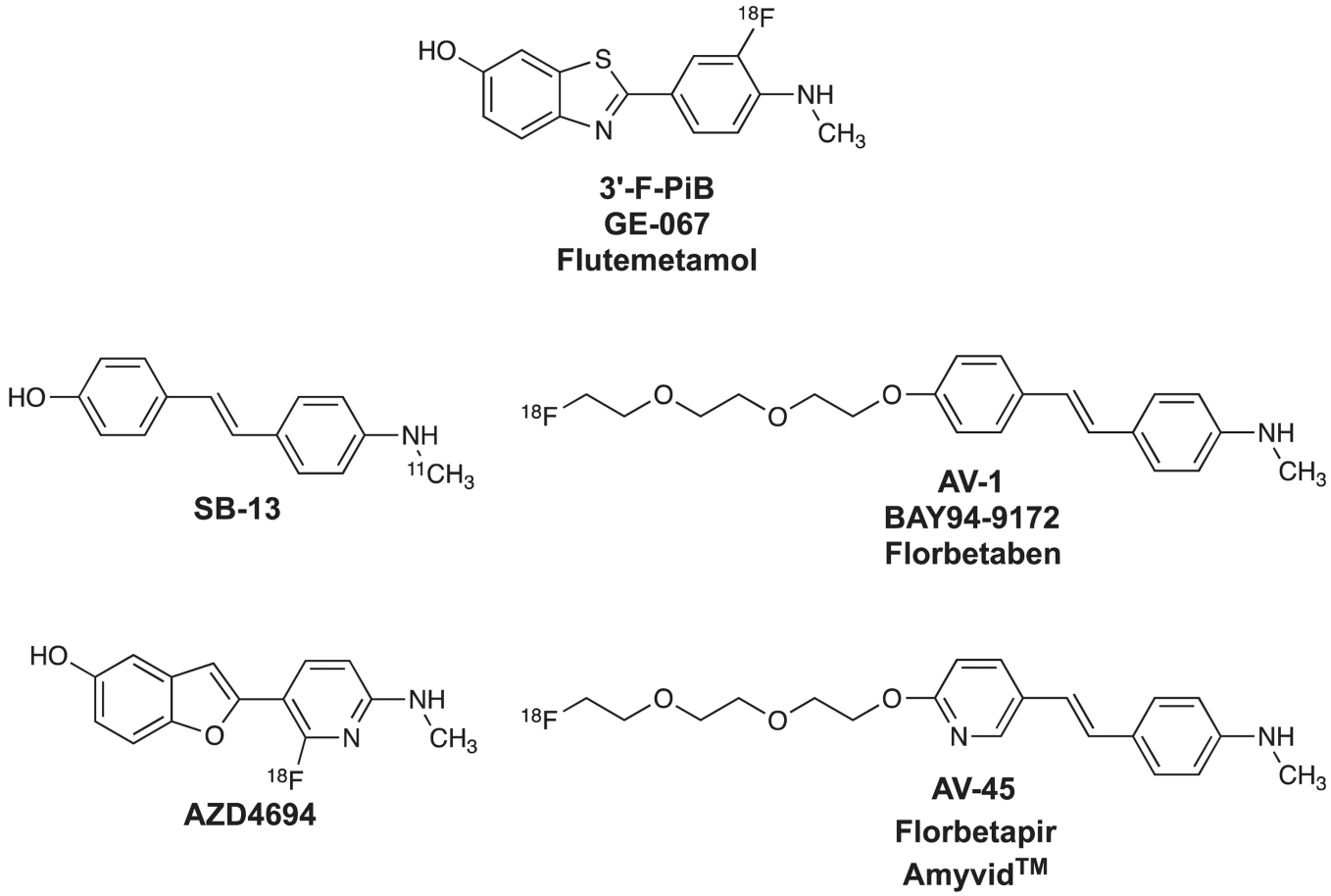

Figure 9.
Structures of different PET radioligands selective for fibrillar Aβ.

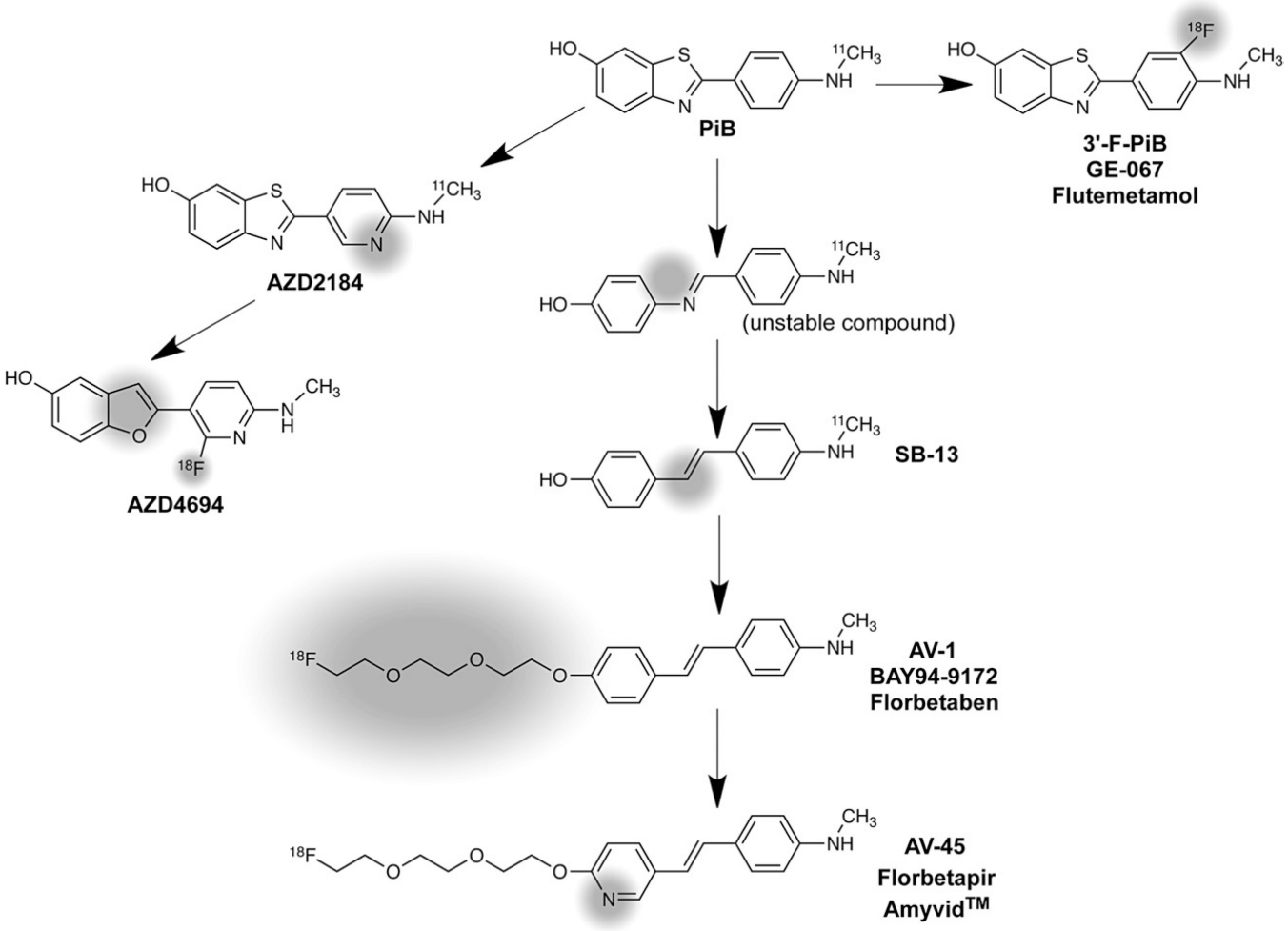

Figure 10.
Evolution from PiB of different Aβ-selective PET radioligands, with significant structural changes highlighted in gray shading.

Table 1

Ideal Properties of an In Vivo Amyloid Imaging Agent

Selectively binds to only amyloid
High affinity for amyloid (K_d ~ 1 nM)
Crosses the blood–brain barrier well at early times after injection (≥0.4%ID/g in rat brain or ≥4%ID/g in mouse brain; may be expressed as a species-independent value where 0.10 (%ID/g) × kg = 100(% ID/g)×g = 1 SUV unit)
Rapid brain clearance of compound not bound to targeted amyloid (clearance $t_{1/2} \leq 30$ minutes in rodents)
No radiolabeled metabolites in brain
Works well in transgenic mice models of AD